Environ Sci Pollut Res (2014) 21:3697–3705
DOI 10.1007/s11356-013-2352-z

RESEARCH ARTICLE

Day–night differences and seasonal variations of chemical species in PM_{10} over Xi'an, northwest China

Zhenxing Shen · Junji Cao · Leiming Zhang · Li Liu · Qian Zhang · Jianjun Li · Yuemei Han · Chongshu Zhu · Zhuzi Zhao · Suixin Liu

Received: 4 June 2013 / Accepted: 6 November 2013 / Published online: 26 November 2013
© Springer-Verlag Berlin Heidelberg 2013

Abstract To investigate day–night differences and seasonal variations of PM_{10} and its chemical composition in an urban environment in Xi'an, northwest China, day- and nighttime PM_{10} mass and its chemical components including water-soluble ions (Na^+, NH_4^+, K^+, Mg^{2+}, Ca^{2+}, F^-, Cl^-, NO_3^-, and SO_4^{2-}), organic carbon (OC), elemental carbon, and water-soluble organic carbon (WSOC) were measured on selected representative days from 20 December 2006 to 12 November 2007. Annual mean PM_{10} concentration in this city was five times of the China Ambient Air Quality Standard for annual average (70 μg m^{-3}). Carbonaceous fractions and water-soluble ions accounted for nearly one third and 12.4 %, respectively, of the annual mean PM_{10} mass. No dramatic day–night differences were found in the loadings of PM_{10} or its chemical components. Spring samples were highlighted by abundance of Ca^{2+}, while the secondary aerosol species (SO_4^{2-}, NO_3^-, and NH_4^+) and OC dominated in summer, autumn, and winter samples. Relatively low NO_3^-/SO_4^{2-} ratio suggested that stationary source emissions were more important than vehicle emissions in the source areas in this city. Strong relationships between WSOC and biomass markers (water-soluble K^+, OC1, and OP) were observed in winter and autumn, indicating that WSOC was derived mainly from biomass burning in these seasons. This was also supported by analysis results on the biomass burning events. In contrast, poor correlations between WSOC and biomass markers were demonstrated in summer and spring, implying that WSOC was mainly formed as secondary organic carbon through photochemical activities.

Keywords PM_{10} · Water-soluble ions · WSOC · Biomass burning · Dust storms

Responsible editor: Gerhard Lammel

Z. Shen · L. Liu · Q. Zhang · Y. Han
Department of Environmental Science and Engineering, Xi'an Jiaotong University, Xi'an 710049, China

Z. Shen (✉) · J. Cao · J. Li · C. Zhu · Z. Zhao · S. Liu
Key Laboratory of Aerosol, SKLLQG, Institute of Earth Environment, Chinese Academy of Sciences, Xi'an 710075, China
e-mail: zxshen@mail.xjtu.edu.cn

L. Zhang
Air Quality Research Division, Science and Technology Branch, Environment Canada, Toronto, Canada

Introduction

PM_{10} (particulate matter with an aerodynamic diameter less than 10 μm) is one of the criteria of air pollutants in China. It is currently indexed in the routine environmental monitoring by the Ministry of Environmental Protection of China (www.zhb.gov.cn/) to estimate air quality. Besides its impacts on environments and climates, PM_{10} and its individual components such as secondary particulate matter are also associated with adverse effects on human health, as has been demonstrated by a large number of epidemiologic studies (Neas 2000; Cao et al. 2012a). Although the new air quality standard in China added daily and yearly $PM_{2.5}$ standard in 2012, PM_{10} is still one of the major indices of air quality. Moreover, considering fugitive dust is one of major components in aerosol particles in semiarid regions, such as the northwest China, PM_{10} is thus a big problem of air quality in these areas. Analysis of respirable particulate matter and its chemical composition can be used to provide scientific basis to determine sources of particulate matter (Wang and Shooter 2001; Duan et al. 2005; Viana et al. 2006; Shen et al. 2011a, b).

Xi'an (34.23° N, 108.88° E) is located in the Guanzhong Plain of a topographic basin surrounded by Qinling

Mountains to the south and the Loess Plateau to the north. Due to its special surrounding topography, days with calmly winds are frequent. This city is now facing increased serious air quality issues due to the rapid increase of motor vehicles (over 1,600,000.00 at the end of 2012) and energy consumption in the past several decades. Earlier studies have suggested that carbonaceous aerosols and water-soluble ions were important components of the TSP/$PM_{2.5}$/PM_1 in Xi'an (Cao et al. 2005a, b, 2007; Shen et al. 2008, 2009a, 2010, 2011a). However, few studies focused on the sequential day–night variations of chemical species in PM_{10} in Xi'an or other cities in China. In this study, 1 year day–night samples were collected in Xi'an and water-soluble inorganic ions, organic carbon (OC), elemental carbon (EC), and water-soluble organic carbon (WSOC) were analyzed. The present study aims to shed some light on the seasonal variations, day–night differences, and sources origins of PM_{10} and its chemical components in an urban environment of Xi'an.

Methodology

Sample collection

The sampling site was located in an urban area of Xi'an (Fig. 1) and was surrounded by residential areas and heavy traffic roads. The sampling campaign was conducted on selected days representing typical seasons or special events which were winter (December 20, 2006 to January 21, 2007), spring (April 1, 2007 to April 29, 2007), summer (July 1, 2007 to July 31, 2007), autumn (October 15, 2007 to November 12, 2007), dust storms (March 31, 2007 and May 4, 2007), and biomass burning (June 10, 2007 to June 12, 2007). A medium-volume PM_{10} sampler (KC-120H, Qingdao Laoshan Electric CO., Ltd., China) was installed on the roof of a 15-m high building. In every 2 days, day- (from 8 a.m. to 6 p.m., Beijing time) and nighttime (from 8 p.m. to next 6 a.m., Beijing time), PM_{10} samples as well as filed blank filters were collected on Φ90-mm quartz microfiber filters (Whatman QMA, England), which were preheated in 900 °C muffle furnace for at least 3 h to avoid inherent carbonaceous contaminants before using. In order to minimize the evaporation of volatile components in PM_{10} samples, the sampled filters were packaged by aluminates paper and stored in a refrigerator at −4 °C until chemical analysis.

Chemical analysis

The mass loadings of PM_{10} samples were determined gravimetrically using a 1-μg sensitivity electronic microbalance (Model MC5, Sartorius AG, Goettingen, Germany). The filters were equilibrated for 24 h at a constant temperature between 20 and 23 °C and relative humidity ranging from 35 to 45 % before weighing. Each filter was weighed three times before and after sampling following the 24-h equilibration period. The mean net mass for each filter was obtained by subtracting the pre-deployment weight from the average of the post-sampling readings. PM_{10} mass concentrations were calculated from the net masses divided by the recorded sampling volumes.

Four anions (SO_4^{2-}, NO_3^-, Cl^-, and F^-) and five cations (Na^+, NH_4^+, K^+, Mg^{2+}, and Ca^{2+}) in PM_{10} samples were determined by ion chromatography (Dionex 600, Dionex Corp, Sunnyvale, USA). Two 0.526-cm^2 punched slices of each quartz filter were extracted by 10 ml distilled–deionized water (resistivity of 18.3 MΩ) in an ultrasonic water bath for 1 h, and then shaken with mechanical shaker for 1 h to completely extract the ionic species. The extracts were filtered with 0.45-mm microporous membrane into a clean vial and stored before analysis. Cations were separated with a CS12A

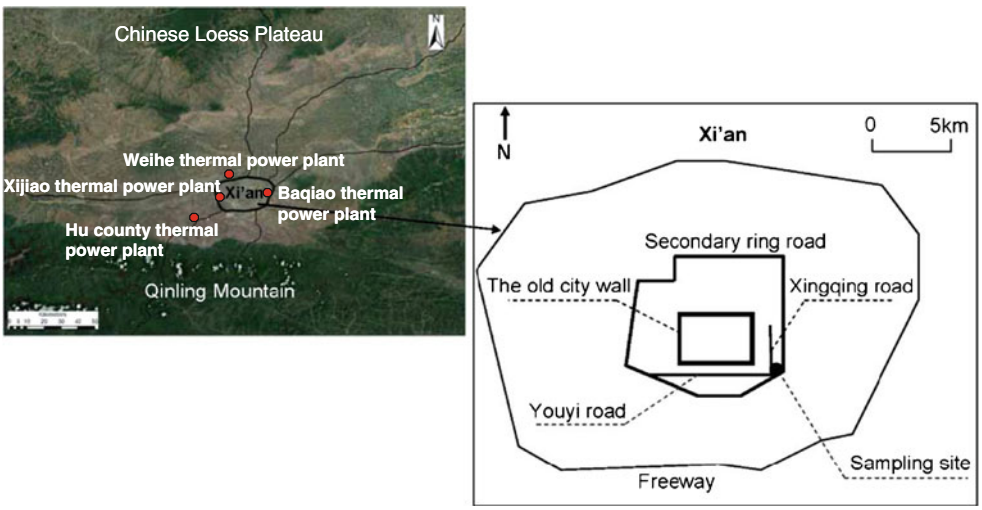

Fig. 1 Location of the sampling site and thermal power plants

column (Dionex Corp.) using 20 mM methanesulfonate as the eluent. Anions were separated by an AS11-HC column (Dionex Corp.) using 20 mM KOH as the eluent. The detection limits were less than 0.05 μg ml^{-1} for all the ions. Standard reference materials produced by the National Research Centre for Certified Reference Materials of China were analyzed for quality assurance purposes. Blank values were subtracted from the total sample concentrations.

OC and EC in PM_{10} samples were analyzed using Thermal and Optical Carbon Analyzer (Model 2001, AtmAA Inc, USA) with Interagency Monitoring of Protected Visual Environment (IMPROVE) thermal/optical reflectance (TOR) protocol. The method produced data for four OC fractions (OC1, OC2, OC3, and OC4 in a helium atmosphere at 140, 280, 480, and 580 °C, respectively), a pyrolyzed carbon fraction (OP, determined when reflected laser light attained its original intensity after oxygen was added to the combustion atmosphere), and three EC fractions (EC1, EC2, and EC3 in a 2 % oxygen/98 % helium atmosphere at 580, 740, and 840 °C, respectively). The IMPROVE protocol defined OC as OC1 + OC2 + OC3 + OC4 + OPC and EC as EC1 + EC2 + EC3-OPC. The carbonaceous analyzer was calibrated with CH_4 every day and repeated analyses were also performed at a rate of one per 10 samples with the difference below 10 %. The detection limits for OC and EC were less than 1.0 μg m^{-3}. The detailed determination procedures of OC and EC together with quality assurance and controls were described in the study of Cao et al. (2003).

Nondispersive infrared absorption TOC analyzer (ET1020A) was used to determine the concentration of WSOC. Pretreated samples together with the purification gas were imported into high-temperature combustion tube and low-temperature reaction tube of organic carbon analyzer, respectively. Water-soluble organic carbon and inorganic carbon in the sample are both transformed into carbon dioxide as a result of high-temperature catalytic oxidation at high-temperature combustion tube. The inorganic carbon was decomposed into carbon dioxide into the low-temperature reaction tube. These two kinds of carbon dioxide generated in the tube were imported to a nondispersive infrared inspection detector. The infrared absorption intensity is proportional to its concentration under a particular wavelength. Total carbon (TC) and total inorganic carbon (TIC) can be determined. The concentrations of WSOC were obtained when TC minus TIC. Before analysis, the PM_{10} samples needed pretreatment. The quartz filters were extracted by 30 ml distilled–deionized water (resistivity of 18.3 MΩ) in an ultrasonic water bath for 1 h and were then shaken with mechanical shaker for 1 h to completely extract the ionic species. The extracts were filtered with 0.45-mm microporous membrane into a clean vial and stored before analysis. Each sample was measured three times; the relative errors of experimental results were between 2.9 and 6.25 %.

Meteorological data

During the sampling periods, hourly meteorological data including ambient temperature, relative humidity (RH), pressure, and wind speed were recorded by the Shaanxi meteorological agency. The meteorological station is located in the northern of Xi'an city, nearly 6 km away from our sampling site.

Results and discussion

Day–night differences of PM_{10} and its chemical components

Daytime PM_{10} levels were slightly higher than those in the nighttime in winter and spring, while the opposite was observed in summer and autumn (Fig. 2). The day–night differences of the detected chemical species seemed to be insignificant. To quantify day–night difference, the coefficient of divergence (CD), a self-normalizing parameter, was applied to compare the spread of the average concentrations of major chemical species. The CD value is calculated as follows:

$$CD_{jk} = \sqrt{\frac{1}{P}\sum_{i=1}^{P}\left(\frac{x_{ij}-x_{ik}}{x_{ij}+x_{ik}}\right)^2} \quad (1)$$

where x_{ij} represents the average concentration for a chemical component i at site j, j and k represent two sampling sites or periods, and p is the number of chemical components. The CDs can be calculated from short-term measurements or long-term averages (Wongphatarakuol et al. 1998; Yang et al. 2005; Shen et al. 2011a, b). A CD approaching zero supports the null hypothesis, which means that the two sampling periods were similar for the measured chemical species. If the differences of aerosol composition between the two sampling periods were significant, CD would approach the unity. In this study, 13 chemical species (PM_{10}, OC, EC, WSOC, Na^+, NH_4^+, K^+, Mg^{2+}, Ca^{2+}, SO_4^{2-}, NO_3^-, Cl^-, and F^-) were used to calculate the CDs for the day- and nighttime.

The calculated CD values for the day–night PM_{10} composition differences were 0.12, 0.14, 0.09, and 0.06, respectively, in spring, summer, fall, and winter (Fig. 3). These small values indicated that the PM_{10} compositions were similar during day- and nighttime. It is noticed that the summer CD value was the highest among the four seasons, indicating the largest difference in aerosol chemical composition between day- and nighttime among all the seasons. The higher CD value in summer than in other seasons might be caused by the more significant differences in sources and meteorology conditions between day and night in this season. As shown in Table 1, daytime O_3 level and temperature (as a surrogate of solar radiation) were much higher than those in the nighttime (Wang et al. 2012). Oxidizing capacity usually associates with solar radiation.

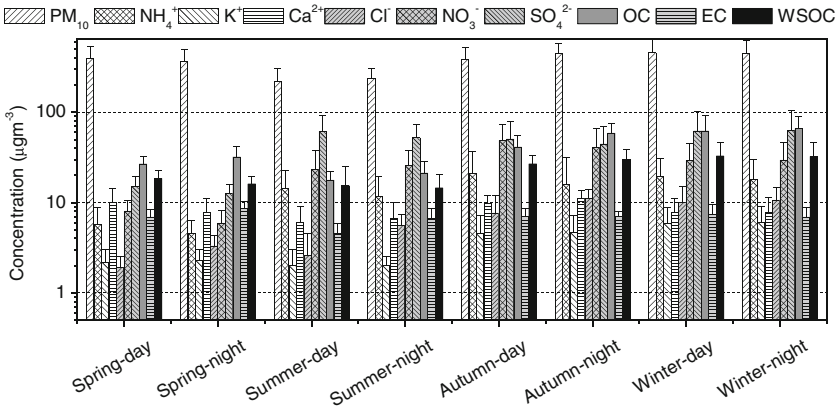

Fig. 2 Day–night variations in chemical components of PM_{10}

Thus, strong solar radiation in summer daytime favors the gas-particle transformation. In comparison, the winter CD value was only about half of the summer value, suggesting similar aerosol components during day and nighttime, which can be explained by the very small day–night differences in O_3, wind speed, and temperature (Table 1, O_3 data was from Wang et al. 2012).

Seasonal variations and source signature of PM_{10} and its chemical components

Seasonal variations of PM_{10} and its chemical components

The mass concentrations of PM_{10} and its chemical components are summarized in Table 2. Annual average PM_{10} concentration reached 366.4 μg m^{-3}, a value that is five times of the China Ambient Air Quality Standard (CAAQS) for annual average (70 μg m^{-3}) and indicates the serious air pollution issues in Xi'an. The PM_{10} levels showed a clear seasonal variation, following the decreasing order of winter >autumn >spring >summer. High winter PM_{10} concentrations should be due to the consumption of the extra coal and biomass in urban and surrounding areas for hearting purposes as well as calmly wind conditions (as shown in Table 1). The observed high sulfate and water-soluble K^+ support this hypothesis. Low summer PM_{10} levels should be mainly attributed to wet scavenging by abundance of precipitation (Shen et al. 2012). As shown in Table 1, summer precipitation amount was about 50 % more than that in autumn and 6 to 12 times higher than in the other two seasons.

Dust storm (DS) events in spring and straw burning events in harvest seasons can cause poor air quality in Xi'an (Cao

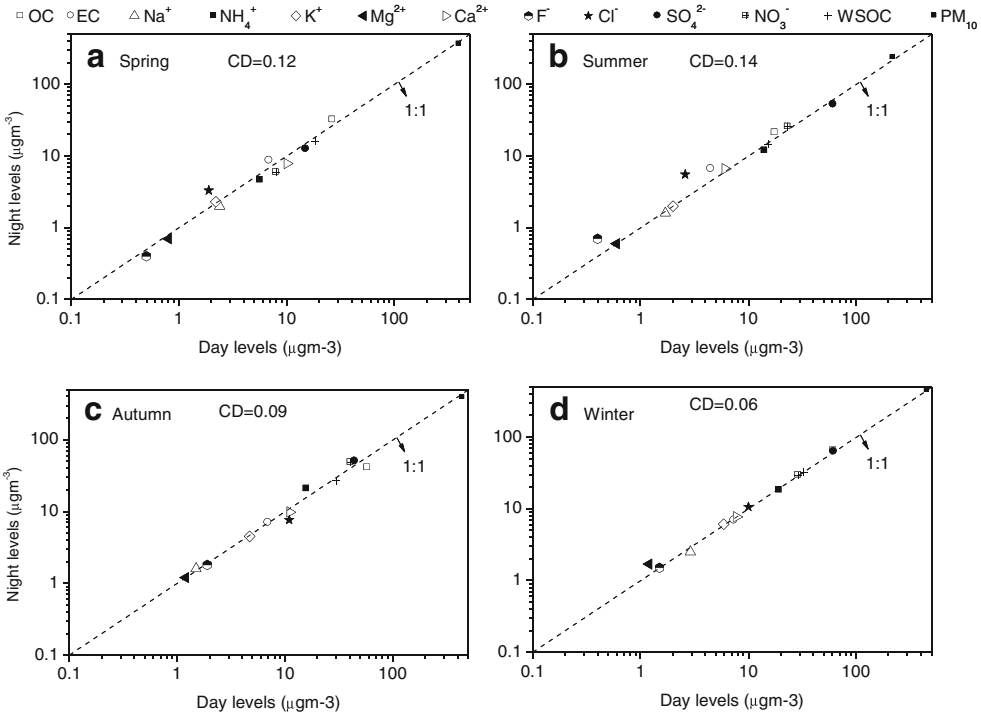

Fig. 3 Comparison of average concentrations of chemical species between day- and nighttime in the four seasons

Table 1 Seasonal variation of meteorological factors and O_3 levels

		Temperature (°C)	RH (%)	Pressure (Pa)	Wind speed (ms^{-1})	Precipitation volume (mm)[a]	O_3 levels (PPBV)[b]
Spring	Day	19.7	43.0	96696.6	2.0	56.8	34
	Night	15.2	56.8	96683.5	1.4		10.8
Summer	Day	28.1	52.2	95988.0	2.0	357.6	47.6
	Night	24.5	63.2	95977.4	1.5		19.4
Autumn	Day	16.7	60.4	97348.0	1.6	216.2	14.7
	Night	13.3	75.7	97371.6	1.2		3.8
Winter	Day	2.7	49.9	98091.0	1.7	29.7	5.4
	Night	0.0	61.8	98129.3	1.2		1.5

[a] Data from Shen et al. (2012)

[b] Data from Wang et al. (2012)

et al. 2005a, b; Shen et al. 2009a), although these events are sporadic. As Xi'an is located on the south margin of Chinese Loess Plateau, DS is a very common phenomenon in spring. Prior literatures reported that heavy DS events in Xi'an led to extremely high PM levels (Cao et al. 2005a, b; Shen et al. 2009a). The burning of wheat straw in summer is also a common method for waste disposal after the crops are harvested on the Guanzhong Plain. Straw combustion in harvest season in suburban areas in Xi'an also causes serious urban air pollution, and the $PM_{2.5}$ level can exceed 400 μg m^{-3} (Shen et al. 2009a). In this study, the mean PM_{10} levels were 1, 018.4 μg m^{-3} for spring DS events and 572.3 μg m^{-3} for summer biomass burning events, respectively, which doubled their respective seasonal mean values.

In general, the total of water-soluble inorganic ions contributed nearly one third of the annual PM_{10} mass. Their percentage contributions varied significantly with season with the highest in summer (45.4 %), followed by autumn (33.5 %), winter (31.0 %), and spring (10.3 %). As Xi'an is located in the semiarid region, spring aerosol was abundant of crustal matters (Cao et al. 2012b), most of which are insoluble materials, such as quartz, aluminosilicate, and feldspar (Shen et al. 2009b). During the dust storm events, total ions occupied only 7.4 % of PM_{10} mass. In contrast, it was 34.2 % in biomass burning samples. SO_4^{2-} level was the highest among all the water-soluble inorganic species in all the four seasons. Seasonal variation of SO_4^{2-} was significant with spring average being only a quarter to a third of those in the other seasons. The highest seasonal average of SO_4^{2-} in winter can be ascribed to coal combustion during heating season. On the other hand, the nearly as high SO_4^{2-} in summer should be linked to strong photochemical transformation processes. Prior studies reported that high temperatures and ozone levels in summer favor the transfer of SO_2 to SO_4^{2-} through heterogeneous reactions (Shen et al. 2008; Wang et al. 2012). The average Ca^{2+} concentration during the spring dust events was three times of the annual mean and during biomass burning events, two times of the annual mean. Ca^{2+} exceeded sulfate in dust events, while the secondary aerosol species (SO_4^{2-}, NO_3^-, and NH_4^+) dominated in total ions in summer, autumn,

Table 2 Statistics summary for the mass concentrations of PM_{10}, water-soluble ions, and carbonaceous species in four seasons (micrograms per cubic meter)

		PM_{10}	Na^+	NH_4^+	K^+	Mg^{2+}	Ca^{2+}	F^-	Cl^-	NO_3^-	SO_4^{2-}	OC	EC	WSOC
Spring	Average	455.1	2.6	4.9	2.3	0.8	11.0	0.5	2.9	7.2	14.7	31.1	8.0	17.2
	SD	254.7	1.6	2.5	0.7	0.4	6.7	0.2	1.4	2.6	4.6	9.3	2.0	4.0
Summer	Average	256.7	1.8	13.5	3.3	0.7	7.3	0.7	5.0	25.7	58.7	25.7	6.6	14.9
	SD	124.4	0.8	8.0	4.7	0.4	4.3	0.6	4.6	13.5	26.8	23.9	4.2	7.8
Autumn	Average	415.9	1.6	18.3	4.6	1.2	10.4	1.8	9.3	44.6	47.4	49.7	7.0	28.3
	SD	129.8	0.6	15.7	2.6	0.4	2.4	0.8	4.1	25.2	26.2	18.0	1.3	7.9
Winter	Average	451.8	2.7	18.8	6.0	1.4	7.7	1.5	10.3	29.3	62.3	63.6	7.1	32.5
	SD	177.1	1.1	11.6	3.0	1.5	3.5	0.7	4.6	16.3	40.8	26.9	2.0	13.5
Year	Average	366.4	2.0	13.8	3.7	1.0	8.3	1.1	6.5	26.3	45.2	40.1	6.8	23.0
	SD	158.3	0.9	11.8	2.6	0.8	3.5	0.8	4.7	21.0	33.3	24.1	2.0	11.5
Dust storm events	Average	1018.4	6.0	2.8	2.8	1.6	26.1	1.1	4.9	8.9	21.2	44.5	10.3	37.2
	SD	201.7	2.1	1.0	0.5	0.2	3.0	0.3	1.6	2.9	4.5	4.1	2.2	2.4
Biomass burning events	Average	572.3	3.8	18.5	17.6	1.6	16.7	1.9	15.3	39.3	81.1	93.4	17.4	57.5
	SD	108.3	0.8	2.7	5.4	0.4	4.3	0.6	9.5	8.0	12.5	39.1	6.4	19.3

and winter samples, the former was caused by natural emissions, while the latter was due to anthropogenic emissions. Prior studies suggested that water-soluble K^+ can be taken as the marker of biomass burning emissions (Andreae 1983; Shen et al. 2009a, b). In this study, water-soluble K^+ concentration during biomass burning (17.6 μg m^{-3}) was five times of the annual mean, which demonstrates that water-soluble K^+ is a good indicator for wheat straw burning.

OC is another important chemical species in PM_{10}. Seasonal variations of OC were as high as a factor of 2.5 with the highest in winter and the lowest in summer. Seasonal variations of EC were less than 20 % with the highest in spring and the lowest in summer. Seasonal pattern of WSOC was similar to that of OC, but the ratio of WSOC/OC exhibited different season pattern with a relatively higher value in summer (averaged, 0.65) and a slightly lower value in winter (averaged, 0.53), implying the varied sources of WSOC in different seasons (more discussions below). The mass of organic matter (OM) was normally calculated as 1.6 times of that of OC (Cao et al. 2003). In this study, carbonaceous species (OM + EC) occupied 12.7, 18.6, 20.8, and 24.1 % of PM_{10} mass in spring, summer, autumn, and winter, respectively. High sulfate combined with high OM in winter indicated the important contributions from coal-burning emissions.

Acidity of PM_{10} and carbonate estimation in spring PM_{10}

Ion balance calculations are useful to evaluate the acid–base balance of particulate matters. The cation and anion microequivalents in the PM_{10} samples were calculated as follows:

$$\mathrm{C(cation\ microequivalents)} = \mathrm{Na^+}/23 + \mathrm{NH_4^+}/18 + \mathrm{K^+}/39 + \mathrm{Mg^{2+}}/12 + \mathrm{Ca^{2+}}/20 \quad (2)$$

$$\mathrm{A(anion\ microequivalents)} = \mathrm{F^-}/19 + \mathrm{Cl^-}/35.5 + \mathrm{NO_3^-}/62 + \mathrm{SO_4^{2-}}/48 \quad (3)$$

where the ion concentrations are in microgram per cubic meter.

Cation and anion equivalents showed a strong correlation (Fig. 4a, $R = 0.89$, $P < 0.0001$) and indicated that the five cations and four anions detected in this study were the major ions extracted from the filters. We noted the slope of the regression line was larger than the unity, implying a deficiency in cations in PM_{10}. Ion balance calculation stratified by seasons showed another important finding (Fig. 4b)—spring and dust storm events samples located below the unity line significantly, indicating alkaline aerosols. The buffering acidity in spring should be due to the high loading of crustal matters. In contrast, summer, autumn, and winter samples positioned above the unity, illustrating acidic aerosols. High levels of sulfate and nitrate should be the major reasons for the particle acidity.

The average ratio (A/C) of total anions versus cations equivalents for PM_{10} samples was 1.03. The seasonal A/C ratios from spring to winter were 0.55, 1.39, 1.13, and 1.11, respectively. It is clear that spring PM_{10} samples were more alkaline, which were mainly due to high loading of dust trace species, such as Ca^{2+} and Mg^{2+}. The imbalances in ions highlighted the fact that not all of the species were determined. In spring, the major fraction of deficit anions should be

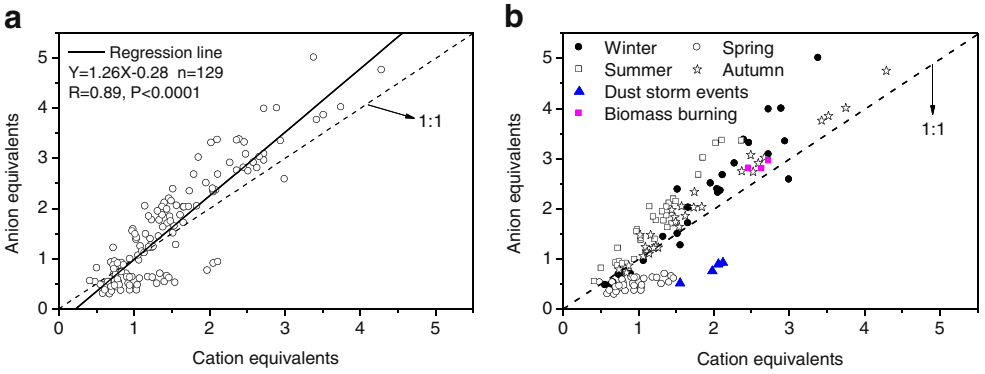

Fig. 4 Total anion microequivalents versus total cation microequivalents for the whole year (**a**) and stratified by seasons (**b**)

carbonate. Prior literatures reported high levels of carbonate in crustal matter during dust storm events (Cao et al. 2005b; Shen et al. 2007, 2009a; Ho et al. 2011). A simple method using ion balance was taken to estimate the carbonate concentration for high dust-loading samples (Shen et al. 2011b). In this study, carbonate concentration (CO_3^{2-}) was estimated to be 14.03 and 35.63 μg m^{-3} in spring PM_{10} and dust storm events samples, respectively. And a strong correlation (R = 0.96, P <0.001) was observed between measured Ca^{2+} and estimated carbonate for the spring PM_{10} and dust storm events samples, indicating the carbonate estimation method used here was reliable. Summer PM_{10} samples showed stronger acidity than autumn and winter samples, which were mainly due to seasonal variations of ion concentrations. In fact, summer PM_{10} showed relatively high levels of acidic species (SO_4^{2-}, NO_3^-, and Cl^-) and low levels of alkaline components (Ca^{2+} and NH_4^+). It was noticed that SO_4^{2-} levels in summer were nearly as high as in winter despite that winter had extra coal burning for heating. Strong solar radiation and high O_3 level in summer should be responsible for this phenomenon as explained above. Prior literatures also revealed that sulfur oxidation ratio (SOR) is much higher in summer than in other seasons (Shen et al. 2008; Wang et al. 2012). The results presented here suggest that PM_{10} can be frequently acidic even in cities of semiarid areas. The seasonal variations in ion mass concentrations suggest that particle acidity was mainly due to SO_4^{2-}, NO_3^-, and Cl^- whereas NH_4^+, Ca^{2+}, and Mg^{2+} were responsible for particles alkalinity.

Source signature for chemical species

SO_4^{2-} mainly originates from stationary sources of coal burning (power plant, industrial, or household burning of coal). As mentioned above, high SO_4^{2-} levels in winter are mainly due to coal burning for heating. In fact, there are four fire-power plants (Xijiao, Baqiao, Weihet, and Hu County) in or closed to Xi'an City (Fig. 1) and residents in suburban areas also used honeycomb briquette in stoves for cooking and heating. The mobile source, mainly referred to vehicle emissions, is the main source of NO_3^-. In literature, the NO_3^-/SO_4^{2-} mass ratio has been sued to evaluate the influences of mobile versus stationary pollution sources (Arimoto et al. 1996; Yao et al. 2002; Shen et al. 2008). A high NO_3^-/SO_4^{2-}mass ratio would indicate the predominance of mobile source over stationary source of pollutants. For example, high mass ratios of 2 and 5 in downtown Los Angeles and in Rubidoux in southern California have been reported (Kim et al. 2000). In this study, NO_3^-/SO_4^{2-} ratio in PM_{10} was 0.59 on average, implying the predominance of stationary emissions in Xi'an. In fact, NO_3^-/SO_4^{2-} ratio in most Chinese cities showed low values (Cao et al. 2012b) due to the coal-dominated energy consumption structure. Decreasing coal consumption and increasing clean energy usage should be the main approach when considering reducing PM levels in China. Seasonal variations in NO_3^-/SO_4^{2-} ratio were also found, and the ratio was 0.5, 0.4, 0.93, and 0.50 from spring to winter, respectively. Besides the seasonal variations of

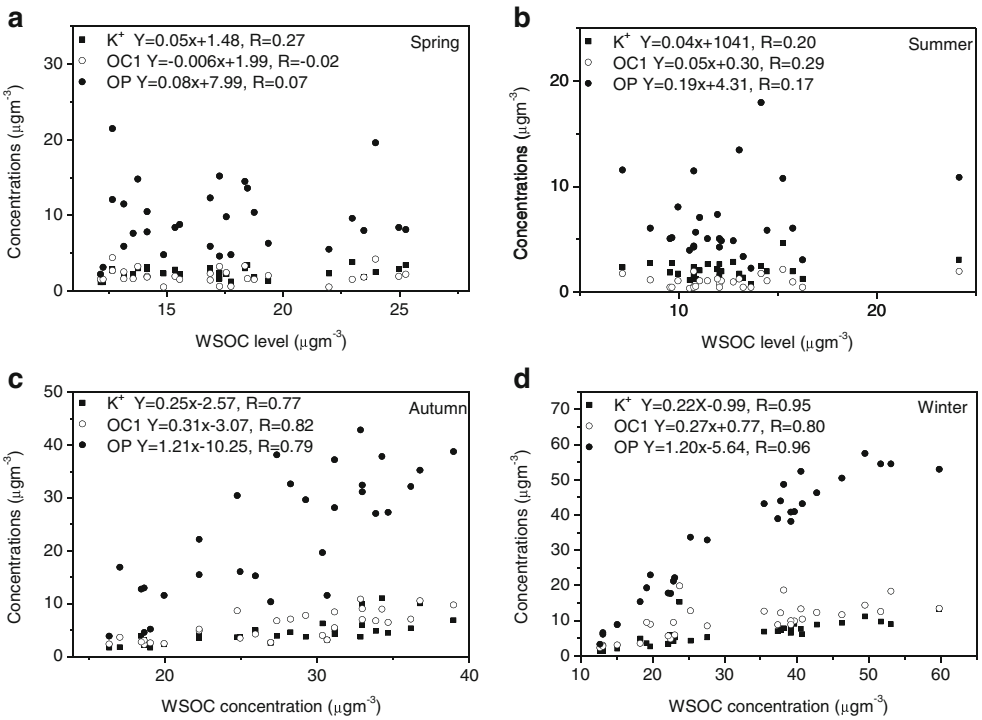

Fig. 5 Correlation between WSOC and biomass burning markers stratified by seasons

emission sources considered above, meteorological conditions might have also contributed to the seasonal variations in the ratio of NO_3^-/SO_4^{2-}. For example, the high NO_3^-/SO_4^{2-} ratio in autumn could be due to the high relative humidity which favored NO_x conversion to NO_3^- (Shen et al. 2008) and the relatively low NO_3^-/SO_4^{2-} ratio in summer might be due to the high temperature which favored SO_2 conversion to SO_4^{2-} (Shen et al. 2008).

The OC/EC ratio can be taken as a tracer of carbonaceous aerosols when the emission sources are relatively stable (Cao et al. 2003, 2005a). The source profile studies of carbonaceous aerosols were still limited in China. Cao et al. (2005a) reported that the OC/EC ratios from coal combustion and biomass burning were much higher than those from motor vehicle emissions. Here, higher OC/EC ratios were observed in autumn and winter (7.1 and 8.9) than those in spring and summer (both averaged, 3.9), inferring the important contribution of biomass burning to autumn and winter samples. In fact, biomass burning in suburban areas of Xi'an was extensive. Wheat straw and maize stalks were burned for cooking year round and for heat during winter and early spring. In addition, wheat straw and maize were burned in field during harvest days leading sporadic pollution events. Samples from biomass burning events also showed a relatively high OC/EC ratio. It is worth to note that EC is normally emitted directly from primary sources, such as fossil fuels combustion, but OC has two types of origins: (1) direct primary emission and (2) secondary process emission such as from homogenous gas-phase oxidation and heterogeneous oxidation. Therefore, the above discussion only qualitatively evaluated the sources of carbon fractions.

Water-soluble organic aerosols (WSOA) are hygroscopic and thus have significant impacts on climate and human health. It is noticed that WSOC occupied half of the OC fraction, which is similar to results from a study in Beijing (Pathak et al. 2011). WSOC usually contains secondary organic carbon (SOC) and/or oxygenated primary organic aerosols, such as diacids, polyols, alcohols, aldehydes, and ketones, and 90 % of WSOC consists oxygenated organic aerosol (OOA) in some regions (Matsui et al. 2009). A major fraction of organic aerosols is water-soluble, accounting for 20–60 % of aerosol carbon mass in fossil fuel combustion-derived particles and 45–75 % in biomass burning-derived particles (Graham et al. 2002; Falkovich et al. 2005; Miyazaki et al. 2006; Pathak et al. 2011). It is important to identify the origins of WSOC before any measures can be taken to reduce it. As shown in Table 1, samples were enriched with WSOC from biomass burning events, followed by winter and autumn samples. As high concentrations of water-soluble K, a biomass burning marker (Shen et al. 2009a, b), were also observed in winter and autumn and biomass burning samples, the contribution of biomass burning to WSOC shodul be important in Xi'an.

Besides K^+, organic carbon fractions, such as OC1 and OP, were also good tracers for biomass burning (Cao et al. 2005a). To further evaluate the sources of WSOC, the correlations of WSOC with selected biomass indicators were conducted here. As shown in Fig. 5, strong positive correlations were revealed between WSOC and water-soluble K, OC1, and OP in winter and autumn samples, indicating winter and autumn WSOC mainly derived from biomass burning emissions. In contrast, poor correlations were extracted in spring and summer samples, inferring other sources, such as photochemical reaction process, instead of biomass burning, should have contributed to WSOC. Pio et al. (2007) revealed that WSOC was largely attributed to the atmospheric oxidation of volatile organic compounds via reactions with strong oxidants (ozone and peroxide radicals) through the gas-phase conversion and the formation of SOA in the atmosphere in nonurban sites in Europe, where biomass burning was limited. Summer and spring WSOC observed in the present study should also be linked with photochemical reaction processes. High ozone levels in summer and spring and low levels in autumn and winter in Xi'an support this assumption. For example, Wang et al. (2012) showed that ozone level was more than ten times higher in summer than in winter. As a result, the origins of WSOC varied by seasons, i.e., biomass burning in winter and autumn and SOC production in summer.

Conclusions

Annual PM_{10} level in Xi'an was 366 μg m^{-3} which was five times of the China Ambient Air Quality Standard (CAAQS) for annual average (70 μg m^{-3}). The identified major components of PM_{10} include sulfate, carbon, crustal matters, nitrate, and ammonium. Day–night differences inPM_{10} and its major chemical components were generally insignificant. High PM_{10}, sulfate, OC, WSOC, and water-soluble K^+ levels in winter were due to coal combustion and biomass burning for heating. High sulfate and WSOC/OC ratio in summer should be attributed to photochemical reaction processes. Spring samples were abundant of crustal matters. The correlation analysis between WSOC and biomass markers (water-soluble K^+, OC1, and OP) concluded that WSOC mainly came from biomass burning in winter and autumn and from photochemical reaction processes in summer and spring. The relatively low NO_3^-/SO_4^{2-} ratio in this study indicated the predominant contribution of coal combustion. Therefore, multipollutant control methods, such as using clear energy to replace the traditional energy, will be needed to alleviate PM pollution levels in Xi'an.

Acknowledgments This research is supported by the Fundamental Research Funds for the Central University of China (grants 2012jdhz38) and the SKLLQG, Chinese Academy of Sciences (grant SKLLQG1213).

References

Andreae MO (1983) Soot carbon and excess fine potassium: long-range transport of combustion-derived aerosols. Science 220:1148–1151

Arimoto R, Duce RA, Savoie DL, Prospero JM, Talbot R, Cullen JD, Tomza U, Lewis NF, Ray BJ (1996) Relationships among aerosol constituents from Asia and the North Pacific during Pem-West A. J Geophys Res 101:2011–2023

Cao JJ, Lee SC, Ho KF, Zhang XY, Zou SC, Fung KK, Chow JC, Watson JG (2003) Characteristics of carbonaceous aerosol in Pearl River Delta region, China during 2001 winter period. Atmos Environ 37(11):1451–1460

Cao JJ, Wu F, Chow JC, Lee SC, Li Y, Chen SW, An ZS, Fung KK, Watson JG, Zhu CS, Liu SX (2005a) Characterization and source apportionment of atmospheric organic and elemental carbon during fall and winter of 2003 in Xi'an, China. Atmos Chem Phys 5:3127–3137

Cao JJ, Lee SC, Zhang XY, Chow JC, An ZS, Ho KF, Watson JG, Fung K, Wang YQ, Shen ZX (2005b) Characterization of airborne carbonate over a site near Asian dust source regions during spring 2002 and its climatic and environmental significance. J Geophys Res. doi:10.1029/2004JD005244

Cao JJ, Lee SC, Chow JC, Watson JG, Ho KF, Zhang RJ, Jin ZD, Shen ZX, Chen GC, Kang YM, Zou SC, Zhang LZ, Qi SH, Dai MH, Cheng Y, Hu K (2007) Spatial and seasonal distributions of carbonaceous aerosols over China. J Geophys Res. doi:10.1029/2006JD008205

Cao JJ, Xu HM, Xu Q, Chen BH, Kan HD (2012a) Fine particulate matter constituents and cardiopulmonary mortality in a heavily polluted Chinese city. Environ Health Perspect 120(3):373–378

Cao JJ, Shen ZX, Chow JC, Watson JG, Lee SC, Tie XX, Ho KF, Wang GH, Han YM (2012b) Winter and summer $PM_{2.5}$ chemical composition in fourteen Chinese cities. J Air Waste Manag Assoc 62:1214–1226

Duan FK, He KB, Ma YL, Jia YT, Yang FM, Lei Y, Tanaka S, Okuta T (2005) Characteristics of carbonaceous aerosols in Beijing, China. Chemosphere 60(3):355–364

Falkovich AH, Graber ER, Schkolnik G, Rudich Y, Maenhaut W, Artaxo P (2005) Low molecular weight organic acids in aerosol particles from Rondonia, Brazil, during the biomass-burning, transition and wet periods. Atmos Chem Phys 5:781–797

Graham B, Mayol-Bracero OL, Guyon P, Roberts GC, Decesari S, Facchini MC, Artaxo P, Maenhaut W, Koll P, Andreae MO (2002) Water-soluble organic compounds in biomass burning aerosols over Amazonia - 1. Characterization by NMR and GC-MS. J Geophys Res 107(D20)

Ho KF, Zhang RJ, Lee SC, Ho SSH, Liu SX, Fung K, Cao JJ, Shen ZX, Xu HM (2011) Characteristics of carbonate carbon in $PM_{2.5}$ in a typical semi-arid area of northeastern China. Atmos Environ 45: 1268–1274

Kim BM, Teffera S, Zeldin MD (2000) Characterization of $PM_{2.5}$ and PM_{10} in the South Coast Air Basin of southern California: Part 1—Spatial variations. J Air Waste Manag Assoc 50:2034–2044

Matsui H, Koike M, Takegawa N, Kondo Y, Griffin RJ, Miyazaki Y, Yokouchi Y, Ohara T (2009) Secondary organic aerosol formation in urban air: temporal variations and possible contributions from unidentified hydrocarbons. J Geophys Res. doi:10.1029/2008JD010164

Miyazaki Y, Kondo Y, Takegawa N, Komazaki Y, Kawamura K, Mochida M, Okuzawa K, Weber RJ (2006) Time-resolved measurements of water-soluble organic carbon in Tokyo. J Geophys Res. doi:10.1029/2006JD007125

Neas LM (2000) Fine particulate matter and cardiovascular disease. Fuel Process Technol 65(66):55–67

Pathak RK, Wang T, Ho KF, Lee SC (2011) Characteristics of summertime $PM_{2.5}$ organic and elemental carbon in four major Chinese cities: implications of high acidity for water-soluble organic carbon (WSOC). Atmos Environ 45:318–325

Pio CA, Legrand M, Oliveira T, Afonso J, Santos C, Caseiro A, Fialho P, Barata F, Puxbaum H, Sanchez-Ochoa A, Kasper-Giebl A, Gelencs´er Schock M, A, Preunkert S, Schock M (2007) Climatology of aerosol composition (organic versus inorganic) at nonurban sites on a west–east transect across Europe. J Geophys Res. doi:10.1029/2006JD008038

Shen ZX, Cao JJ, Arimoto R, Zhang RJ, Jie DM, Liu SX, Zhu CS (2007) Chemical composition and source characterization of spring aerosol over Horqin sand land in northeastern China. J Geophys Res. doi:10.1029/2006JD007991

Shen ZX, Arimoto R, Cao JJ, Zhang RJ, Li XX, Du N, Okuda T, Nakao S, Tanaka S (2008) Seasonal variations and evidence for the effectiveness of pollution controls on water-soluble inorganic species in total suspended particulates and fine particulate matter from Xi'an, China. J Air Waste Manag Assoc 58:1560–1570

Shen ZX, Cao JJ, Arimoto R, Han ZW, Zhang RJ, Han YM, Liu SX, Okuda T, Nakao S, Tanaka S (2009a) Ionic composition of TSP and $PM_{2.5}$ during dust storms and air pollution episodes at Xi'an, China. Atmos Environ 43:2911–2918

Shen ZX, Caquineau S, Cao JJ, Zhang XY, Han YM, Gaudichet A, Gomes L (2009b) Mineralogical characteristics of soil dust from source regions in northern China. Particuology 7:507–512

Shen ZX, Cao JJ, Arimoto R, Han YM, Zhu CS, Tian J, Liu SX (2010) Chemical characteristics of fine particles (PM_1) from Xi'an, China. Aerosol Sci Technol 44:461–472

Shen ZX, Cao JJ, Liu SX, Zhu CS, Wang X, Zhang T, Xu HM, Hu TF (2011a) Chemical composition of PM_{10} and $PM_{2.5}$ collected at ground level and 100 meters during a strong winter-time pollution episode in Xi'an, China. J Air Waste Manag Assoc 61:1150–1159

Shen ZX, Wang X, Zhang RJ, Ho KF, Cao JJ, Zhang MG (2011b) Chemical composition of water-soluble ions and carbonate estimation in spring aerosol at a semi-arid site of Tongyu, China. Aerosol Air Qual Res 11:360–368

Shen ZX, Zhang LM, Cao JJ, Tian J, Li L, Wang GH, Zhao ZZ, Wang X, Zhang RJ, Liu SX (2012) Chemical composition, sources, and deposition fluxes of water-soluble inorganic ions obtained from precipitation chemistry measurements collected at an urban site in northwest China. J Environ Monit 14:3000–3008

Viana M, Chi X, Maenhaut W, Querol X, Alastuey A, Mikuska P, Vecera Z (2006) Organic and elemental carbon concentrations in carbonaceous aerosols during summer and winter sampling campaigns in Barcelona, Spain. Atmos Environ 40(12):2180–2193

Wang HB, Shooter D (2001) Water-soluble ions of atmospheric aerosols in three New Zealand cities: seasonal changes and sources. Atmos Environ 35(34):6031–6040

Wang X, Shen ZX, Cao JJ, Zhang LM, Liu L, Li JJ, Liu SX, Sun YF (2012) Characteristics of surface ozone at an urban site over Xi'an in northwest China. J Environ Monit 14:116–126

Wongphatarakuol V, Freidlander SK, Pinto JP (1998) A comparative study of $PM_{2.5}$ ambient aerosol chemical database. Environ Sci Technol 32:3926–3934

Yang FM, Ye BM, He KB, Ma YL, Cadle SH, Chan T, Mulawa PA (2005) Characterization of atmospheric mineral components of $PM_{2.5}$ in Beijing and Shanghai, China. Sci Total Environ 343: 221–230

Yao XH, Chan CK, Fang M, Cadle S, Chan T, Mulawa P, He KB, Ye B (2002) The water-soluble ionic composition of $PM_{2.5}$ in Shanghai and Beijing, China. Atmos Environ 36:4223–4234